A NUMERICAL MODEL OF THE EFFECTS OF REACTOR COOLING WATER ON FJORD CIRCULATION (I)

by Wayne Wilmot

SMHI Rapporter

HYDROLOGI OCH OCEANOGRAFI

Nr RHO 6 (1976)

SVERIGES METEOROLOGISKA OCH HYDROLOGISKA INSTITUT

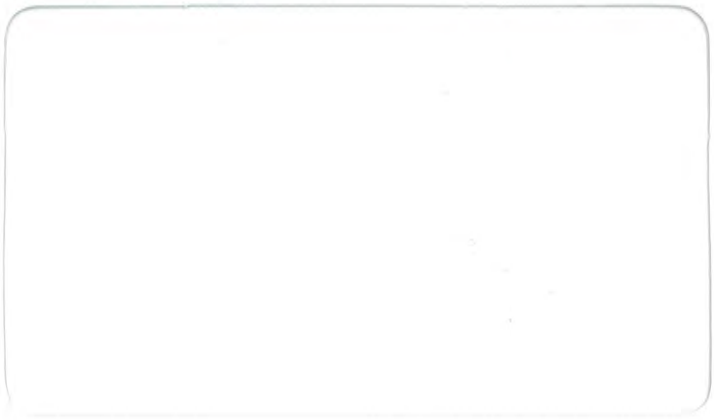

A NUMERICAL MODEL OF THE EFFECTS OF REACTOR COOLING WATER ON FJORD CIRCULATION (I)

by Wayne Wilmot

SMHI Rapporter

HYDROLOGI OCH OCEANOGRAFI

Nr RHO 6 (1976)

EN NUMERISK MODELL ÖVER EFFEKTERNA AV REAKTORKYLVATTEN PÅ FJORDCIRKULATION

SVERIGES METEOROLOGISKA OCH HYDROLOGISKA INSTITUT

Norrköping 1976

CONTENTS

ABSTRACT

In the search for possible sites for new nuclear power plants in Sweden a site on Bråviken, a narrow fjord, is being considered. A numerical hydrodynamic model has been developed to predict the probable effects of the waste heat discharged into the estuary on the natural estuarine flow.

The model employs the basic equations of motion and conservation of salt and heat with appropriate approximations to make predictions. The primary approximation in the model consists of considering the estuary as a channel in which cross channel effects do not explicitly appear. The along channel motion is thus primary determined by the along channel density gradients.

A number of different cases have been investigated. The basic states in the summer and in the winter have been established in order to evaluate effects of heated water in two different conditions of thermal stratification. For each of these seasons two different intake configurations have been considered: a surface intake and a bottom intake. The outlet is located at the surface. The above situations have been considered for several wind conditions: no wind, a 5 m/s constant wind tending to transport water into the estuary, and a 12 m/s time dependent wind which gradually builds up blowing out of the estuary, changes direction and then dies away. A series of experiments with various runoff values at the head of the fjord have been conducted.

With the construction of a bottom intake located at the depth of about 40 meters there will be little noticable effect on the circulation, temperature or salinity fields in the estuary in the summer. However in the winter the bottom intake offers only a partial improvement over a surface intake. During the winter the heated water would cause changes of as much as 50 % in the natural state. The surface intake would cause changes which sometimes are almost twice as big. The problem arises because the 10°C heated water creates sizable horizontal density gradients which are sufficient to counteract the weak natural flow.

ACKNOWLEDGEMENTS

I would like to thank Ulf Ehlin of SMHI for his support of this work. I am grateful to Jonny Svensson of SMHI for his many suggestions and criticisms at all stages of this project.

1. INTRODUCTION

There have been proposals in Sweden to increase electrical energy production by building more nuclear power plants. These plans include proposals to build reactors at new sites as well as at existing ones. This study has been initiated as part of an investigation into the environmental impact of a nuclear power station planned for a new site near Tunaberg on Bråviken. Bråviken is a fjord-like estuary on the East coast of Sweden about 200 kilometers south of Stockholm.

Thermal power plants employ various sources to produce heat which is converted, in a steam turbine, to electrical energy. The efficiency level of such energy production runs between thirty and forty percent. The remaining sixty to seventy percent of the heat is a waste product of electrical energy production and must be disposed of in the environment. The proposed nuclear power station at Tunaberg is designed to dispose of the heat into water drawn from Bråviken estuary. The heated water is returned to the estuary at a point several kilometers from the intake. The site is investigated for a power plant with six aggregates with a heat rejection of 12 500 MW. In one month's time, a volume of water equal to the total volume of Bråviken would pass through the reactor condenser stage and be returned to the environment with a temperature 10°C higher than it had upon entering. Such waste heat, deposited into the estuary, may be considered as thermal pollution in the sense that it constitutes a thermal stress on the ecology of the estuary. The most obvious stress is that due to extreme temperatures. A recent (Kylvatten-effekter på miljön. Ehlin et. al. 1974. Statens Naturvårdsverk Publikationer 1974:25) study of temperature stresses at a thermal power station found that wind driven currents could trap outlet water in a small bay and cause temperature rises of over 10°C within several hours. Such thermal stress is very detrimental to the biological life of the estuary.

Thermal pollution of the magnitude that results from nuclear power plants is not merely a passive pollutant. The heated water effluent constitutes a huge excess of buoyancy located near the outlet. A circulation can be driven by the large horizontal density differences. The so called "estuarine" circulation in an estuary is driven by heat and salt gradients along the estuary. These gradients are maintained by natural sources of buoyancy such as runoff and solar radiation. Thermal pollution could change, perhaps favorably as well as unfavorably, the natural circulation. In addition to the weak density driven circulation, there are currents associated with surface wind stresses. The wind driven currents have by far the larger amplitude and are highly time dependent. However, they have very little net effect on the average conditions in an estuary. The transport of nutrients and oxygen to the deeper waters of the estuary is largely dependent on the slow estuarine circulation. The estuarine circulation is influenced to some degree by the wind driven currents but to a greater extent by fluctuations in buoyancy sources. This study is intended to make predictions of the effects of the planned reactor on the estuarine circulation as well as the possible thermal stress imposed on the ecology of the estuary.

Once the "cooling" water is re-introduced into the estuary, the heat it contains is either mixed with and advected in the waters of the estuary, or is lost to the atmosphere. Usually the outlet is designed to mix the heat with the ambient water as rapidly as possible by using a high velocity jet. Sometimes a submerged diffuser is used to enhance the turbulent mixing of a rising buoyant plume. This type of enhanced mixing is intended to reduce the overtemperature. The overtemperature is the temperature rise above the natural level due to the heated water effluent. The near field, that is, within a kilometer or so of the outlet, is dominated by mixing processes associated with the outlet jet. By vigorously mixing the heated water with the surrounding water, the exchange to the atmosphere is highly reduced. Atmospheric exchange processes are strongly dependent on the temperature. In some power plant designs, the philosophy has been to enhance exchange to the atmosphere, making it the immediate recipient of the excess heat. Cooling towers are designed for this purpose. Enclosed bodies of water, cooling ponds, are used as well, to provide a large surface area for exchange to the atmosphere. The use of the estuary as a heat recipient is very different from the use of a cooling pond. In the case of the estuary, the water is to be the ultimate recipient and storage place for the heat. In order to take advantage of the large heat capacity of the seas, it is necessary to have a free exchange of water containing the waste heat with the great volume of sea water available. It is important to determine whether a site chosen for basically industrial reasons is appropriate for the disposal of excess heat. In addition to the environmental considerations, there are those of plant efficiency. If the estuary becomes stagnated for a period of time, then the excess heat will not be transported to the sea. Instead, it will be recirculated through the plant reducing the efficiency of the energy production. Variable wind driven currents could contribute to recirculation during the time wind drives flow from the outlet to the intake. Since the design of the Tunaberg plant is based on the idea of using Bråviken and eventually the whole Baltic as a heat recipient, it is important to understand whether this premise is feasible.

This study concerns itself with scales which are related to the far field, that is, those scales associated with natural mixing, advection and atmospheric transfer processes. The questions are therefore; what effect does the excess buoyancy have on the circulation of the estuary and how large an excess temperature can be expected in various parts of the estuary under reasonable conditions?

There are several approaches which can be taken to answer these questions. One possibility is the construction of a physical model of Bråviken which extends offshore into the undisturbed Baltic. The model should end at the point in the Baltic where the flow is independent of the heated water effluent. Along these lines, a model of the limited area around the intake-outlet region has been constructed. However, it does not cover any of Bråviken itself and has three of its four sides open to non interactive water. The boundaries are located in a region where the flow is

still influenced by the heated water plume. This model cannot hope to answer the questions above. What it may do is show how effective the outlet jet is in mixing the heat with the ambient water. It is an approach to nearfield problems but is not concerned with the ultimate fate or impact of the heat. To study that, a physical model covering a much larger area would be necessary. A model in which details of topography have been sacrificed for extended coverage would be more appropriate and useful in answering the broader questions.

A computer "jet" model of the effluent has been used to estimate the overtemperatures in the plume. But again, it is for use in the near field only and assumes that currents act only to increase mixing of the heat and to advect heat from the nearfield region. It does not attempt to answer any questions about the ultimate fate and influence of the heat.

A two dimensional finite difference grid numerical model has been employed in the present study to predict the large scale circulation and heat transport in Bråviken due to the heated water. It should be emphasized that the scales and processes considered here are those of the environment and not those of the outlet jet. It is assumed that the engineer has accomplished his goal and effectively mixed the heated water into the estuary. The smallest horizontal scale considered in the numerical model is on the order of a kilometer. This is about the maximum distance from the jet in which jet induced mixing and entrainment dominate.

In addition to these models field work is being done to determine what constitutes natural environmental conditions in Bråviken. The field work is not in itself a prediction of the impact of the proposed reactor, but provides necessary information for evaluation of the models as well as providing substance for intuitive predictions.

2. BRÅVIKEN

2.1 Topography

As part of the study of Tunaberg as a possible site for a nuclear power plant, field studies are being performed. The measurements have been done concurrently with the numerical work and have not been available for input to any extent into this model. However, existing routine field measurements near Bråviken have provided the basis for model idealizations.

The general topography of Bråviken (Figure 2.1) has been adapted from the Swedish nautical charts. The representation of the topography has been simplified somewhat since the numerical model does not represent longitudinal scales less than one kilometer. The region of major importance is the main channel, as defined by the 10 m depth contour, which runs along the north coast of Bråviken. The sill is located at Järknö with a depth of about 21 meters. The maximum depth of the channel is about 50 meters. The planned sites of the intake and outlet are shown in Figure 2.1. The sites are adjacent to the deep channel. The large area to the south is rather shallow and has many islands.

The width of the channel perpendicular to the center of the deepest part of the channel is of importance to the numerical model. Contours of equal width, Figure 2.2, have been taken at at spacing equal to the model grid spacing. The grid spacing is one kilometer in the horizontal and one meter in the vertical. A smoothed width function has been used for the computations. The width, $b(x,z)$, was expressed as a function of the depth, z, the maximum depth, $h(x)$, and the longitudinal coordinate x as:

$$b(x,z) = b(x,z = 10 \text{ meters}) \cdot \left(1 - \sin \frac{z\,\pi}{h(x)}\right) \qquad (2.1)$$

The variation of volume with depth is plotted in Figure 2.3.

2.2 Runoff

The major source of fresh water in Bråviken is runoff from the Motala river, entering at the head of the estuary. Figure 2.4 shows the maximum, minimum and mean fresh water runoff during the period 1935-1975. Also shown are the runoff data from 1949 and 1973, both chosen as years of low runoff. In 1973, the average runoff was about 50 m^3/s and the smallest value was 25 m^3/s. The largest runoff value during the entire 40 year period was about 300 m^3/s. All data points are monthly means.

Precipitation contributes at the most about 5 m^3/s over the whole estuary. This is balanced over the course of a year by evaporation.

2.3 Water Level

Monthly water level variations in Bråviken for 1973-1974 are shown in Table 2.1. The energy spectra for the time series of water level data shows a peak at about 5 hours. Volume transports

associated with these oscillations are less than fluctuations in runoff and wind driven transports.

Tabel 2.1. Water level, cm

Month, year	Max	Min	Mean
December, 1974	67	0	35
November	36	-12	7
October	39	-8	10
September	18	-24	-3
August	35	-7	10
July	42	3	22
June	12	-16	0
May	-1	-47	-32
April	-12	-48	-31
March	-8	-55	-37
February	17	-18	0
January	28	-23	3
December, 1973	68	3	31
November	73	-27	21
October	25	-19	-5
September	34	-22	4
August	14	-15	1
July	21	-12	1
June	16	-22	-6
May	12	-23	-8
April	28	-13	8
March	17	-22	0
February	30	-24	11
January	18	-44	-12

2.4 Wind

The wind frequency diagram in Figure 2.5 comes from data taken at Studsvik on the east coast near Bråviken. The data indicates that the wind is under 5 m/s about 80 % of the time.

2.5 Temperature and Salinity at Baltic Boundary

Temperature and salinity along a longitudinal section through Bråviken are available for August 1973 and November 1973 to compare with numerical simulation of the natural state (Figures 5.1, 5.2, 5.28 and 5.29). The section runs along the deep channel of Bråviken from Motala Ström to Grässkären. Data taken from the hydrographic station at Grässkären, August 1973 and November 1973 have been used to establish the boundary conditions at the Baltic side of the model. The data shown in Figure 2.6 are typical for summer and winter thermal stratification states.

3. MATHEMATICAL FORMULATION

3.1 Basic Approximations

The governing hydrodynamical equations express the velocity and density fields as functions of space and time. Even in their complete form they merely represent approximations to nature. Turbulence can be formally represented by an infinite set of coupled equations. It is impractical, however, to look for solutions to any but the lowest few orders of turbulent equations. The turbulent equations are often avoided entirely by assuming that the turbulence acts in a way analogous to molecular processes. Turbulent diffusion is then represented as the product between an eddy coefficient and the mean gradient. The understanding of mixing processes in estuaries has proceeded only to the point of representing such coefficients as functions of the mean fields. The model presented here does not attempt to go beyond this simple representation of turbulence. The scaling of the basic equations gives an idea of which processes predominate. The equation of vertical motion in estuaries can be represented quite accurately by the hydrostatic balance. That is to say that vertical momentum is unimportant. The vertical pressure gradients adjusts itself to the density field. Furthermore, density variations are only important in the momentum balance through the horizontal pressure gradient. The density can be considered as a constant when multiplying the accelerations or friction terms. The flow is incompressible making the velocity field non-divergent. The vertical velocity enters in order to account for divergences in the horizontal flow. Vertical flow is essential for the transport of salt, heat and horizontal momentum in estuaries.

Further simplification of the equations can be achieved by applying knowledge of estuarine circulation obtained from field observations. It is often observed in long narrow fjord type estuaries that the predominant gradients run along the channel. The cross channel gradients are much smaller. This is often due to the fact that major rivers empty into the estuary near the head. Bråviken is of this type. This situation allows for a reduction in the number of space coordinates. The salt and heat equations can be averaged across the channel. The momentum equations along and across the channel can be decoupled by assuming that the cross channel velocity is much smaller than the velocity along the channel. This could be viewed as a canal model in which the velocity along the channel is accelerated or decelerated by width variations.

The equations remaining, after all of the above simplifications have been made, are still non linear and quite difficult to solve analytically. The salt, heat and vorticity equations are time dependent and non linear. The continuity equation and non-linear equation of state complete the set of equations to be solved.

It has been assumed that the barotropic response of the basin is independent of the internal density field. That is, the water level variations due to runoff, rain, atmospheric pressure disturbances and wind stress are not influenced by the density field. These barotropic responses are used as known forcing functions. They are imposed as vertical velocities on a level rigid lid.

3.2 Coordinates and Variables

A right hand coordinate system is used such that x is directed along the estuary, y across the estuary and z down in the direction of the gravitational acceleration (Figure 3.1). The width of the estuary, b(x, z), is a function of position in the longitudinal and vertical directions. The velocity components u, v, w are in the x, y, z directions respectively. The depth, h(x), is a function of the longitudinal coordinate.

3.3 Dynamical Balance

A Boussinesq dynamical balance is considered along the vertical-longitudinal plane of the estuary. The density variations do not affect the accelerations or frictional terms. The cross channel balance can be approximated by geostrophy (Pritchard, 1956, Stewart, 1957), in which the pressure gradient adjusts itself to variations in the long channel flow. The vertical accelerations are negligible and the pressure gradient adjusts itself to variations in the density field. The longitudinal momentum equation can be written as,

$$\frac{\partial u}{\partial t} + u\frac{\partial u}{\partial x} + w\frac{\partial u}{\partial z} = -\frac{\partial \pi}{\partial x} + \frac{\partial}{\partial x}\left(A_h \frac{\partial u}{\partial x}\right) + \frac{\partial}{\partial z}\left(A_v \frac{\partial u}{\partial z}\right) \qquad (3.1)$$

where π is the pertubation pressure which remains after the hydrostatic pressure due to water of a constant density, ρ_o, is substracted and A_h, A_v are the horizontal and vertical eddy viscosities. The coriolis acceleration, $-fv$, as well as the lateral advection of lateral shear, $v\frac{\partial u}{\partial y}$, are eliminated by making the canal assumption. The cross channel velocity, v, and its derivative, $\frac{\partial v}{\partial y}$, is negligible at the center of the channel. It is present at the sides in order to allow for acceleration and deceleration of the flow due to width variations. It does not contribute to the long channel dynamics, however.

The cross channel geostrophic balance can be written as,

$$fu = -\frac{\partial \pi}{\partial y} \qquad (3.2)$$

where f is the coriolis parameter, $f = 2\Omega \sin \phi$, Ω = earth's rotation rate, ϕ = the latitude. The lateral momentum equation simply expresses the fact that the lateral pressure gradient adjusts geostrophically to variations in the long channel flow.

The boundary condition for the vorticity equation on the open oceanic boundary is that the vorticity be continuous,

$$\frac{\partial \eta}{\partial x} = 0 \qquad (3.9)$$

This implies, through continuity, that the vertical shear of the vertical velocity is a constant on that boundary. The contribution to the vertical velocity of the density field is zero. The vertical velocity is linear with depth and is due to depth variations affecting the barotropic flow alone. In other words, the outer boundary is in an oceanic region where the density flow is essentially horizontal.

The vorticity is predicted by the vorticity equations and appropriate boundary conditions. The vorticity is added to the estuary through wind stress at the surface and frictional stress at the bottom. Vorticity is generated internally by horizontal density gradients due to heat sources and dilution by fresh water. Vorticity is advected by the flow and diffused by turbulent viscosities.

3.4 Continuity Equation

The approximation of incompressibility implies that the flow is non-divergent. When the continuity equation in three dimensions is integrated across the channel (Pritchard, 1958) and the kinematic boundary conditions are applied, the following equation results,

$$\frac{\partial}{\partial x}(bu) + \frac{\partial}{\partial z}(bw) = 0 \qquad (3.10)$$

The continuity equation (3.10) is identically satisfied if we define a transport stream function, Ψ ,

$$bu = -\frac{\partial \Psi}{\partial z}$$
$$bw = +\frac{\partial \Psi}{\partial x} \qquad (3.11)$$

The vorticity is given by the equation,

$$\eta = \frac{\partial}{\partial z}\left(\frac{1}{b}\frac{\partial \Psi}{\partial z}\right) \qquad (3.12)$$

The stream function is found by vertical integration of equation (3.12) and by application of the boundary conditions on the flow. The stream function is given on the bottom and at the surface,

$$\Psi = \Psi_B(x) \qquad z = h(x)$$
$$\Psi = \Psi_S(x, t) \qquad z = 0 \tag{3.13}$$

The streamfunction, Ψ_B, is zero on the bottom unless there is a bottom intake. In that case there is a jump at the intake from zero to a constant, representing the intake transport. The streamfunction at the surface is due to the runoff transport, meteorological time dependent transports and the reactor cooling water intake and outlet system (Figure 3.3). The difference between the streamfunction at the surface and at the bottom in any vertical column is the barotropic transport (specified) through that section. The flow is obtained when equation (3.12) is integrated. The flow depends on the density structure through the vorticity generation term in equation (3.4).

3.5 Salt Conservation

The salt conservation equation in three dimensions can be averaged across a channel of width b(x, z), (Pritchard, 1958), by assuming lateral homogeneity. The resulting salt equation (Figure 3.4) is given by,

$$b\frac{\partial S}{\partial t} + \frac{\partial (buS)}{\partial x} + \frac{\partial (bwS)}{\partial z} = \frac{\partial}{\partial x}\left(bK_h^S \frac{\partial S}{\partial x}\right) + \frac{\partial}{\partial z}\left(bK_v^S \frac{\partial S}{\partial z}\right) \tag{3.14}$$

where S is the salinity and K_h^S, K_v^S are the horizontal and vertical eddy diffusivities of salt.

There are no advective or diffusive fluxes of salt through the bottom in the absence of an intake:

$$u_n S = 0$$
$$\frac{\partial S}{\partial n} = 0 \qquad z = h(x) \tag{3.15}$$

where n indicates the normal direction to the boundary. With a bottom intake, the flux is due to the advective flux, wS.

$$\text{Net flux} = -K_v^S \frac{\partial S}{\partial z} + wS = (wS)_{\text{intake}}, \quad z = h(x) \tag{3.16}$$

At the surface, the net flux of salt is zero in the absence of an intake or outlet.

$$\text{Net flux} = -K_v^S \frac{\partial S}{\partial z} + wS = 0, \quad z = 0 \tag{3.17}$$

This guarantees that there is no loss or gain of salt through the surface even with a water transport (runoff or meteorological). At an intake, however, the net flux out of the estuary

is equal to $(wS)_{intake}$. At the outlet point the net flux is equal to the flux into the inlet. The time for passage through the cooling system is about 2 hours and can be viewed as almost instantaneous when compared to the time scales of importance in the model.

The boundary condition at the oceanic side is not obvious. There is no clear point at which the effect of the estuary on the Baltic can be considered to end. If the observed vertical salinity distribution is specified, a problem occurs in the regions of outflow where the outgoing water carries a different salinity than the one specified. An unrealistic horizontal boundary layer results and the interior solution is greatly in error. Instead, only the salinity of the inflowing water is specified. The horizontal gradient of salinity is set to zero in outflowing regions:

$$\begin{aligned} S &= S_o(z, t), \quad u \leq 0 \\ \frac{\partial S}{\partial x} &= 0, \qquad u > 0 \end{aligned} \tag{3.18}$$

The flow at this boundary is determined as a function of depth and time from integration of equation (3.12).

The predictive equation for salinity states that the time change of salinity is due to advection and turbulent diffusion (Figure 3.4). Dilution by fresh water maintains the horizontal salinity gradients. The fresh water source is at the surface and so tends to stably stratify the estuary. The only destabilizing effect is due to the discharge of bottom intake water which has a higher salinity than the surface water into which it is discharged.

3.6 Heat Conservation

The heat conservation equation (Figure 3.5) is derived in a similar way to the salt equation and is written,

$$b\frac{\partial T}{\partial t} + \frac{\partial (buT)}{\partial x} + \frac{\partial (bwT)}{\partial z} = \frac{\partial}{\partial x}\left(bK_h^T \frac{\partial T}{\partial x}\right) + \frac{\partial}{\partial z}\left(bK_v^T \frac{\partial T}{\partial z}\right) \tag{3.19}$$

where T is the temperature and K_h^T, K_v^T are the horizontal, vertical eddy diffusivities of heat.

There are no advective or diffusive fluxes of heat through the bottom in the absence of an intake:

$$\begin{aligned} u_n T &= 0 \\ \frac{\partial T}{\partial n} &= 0 \end{aligned} \qquad z = h(x) \tag{3.20}$$

where n indicates the normal direction to the boundary. With a bottom intake the flux is due to the advective flux, wT.

$$\text{Net flux} = -K_v^T \frac{\partial T}{\partial z} + wT = (wT)_{\text{intake}}, \quad z = h(x) \tag{3.21}$$

At the surface the net flux of heat is Q_{net} in the absence of an intake or outlet,

$$\text{Net flux} = -K_v^T \frac{\partial T}{\partial z} + wT = \frac{Q_{net}}{\rho_o C_P} \tag{3.22}$$

where C_P is the specific heat at constant pressure. The net source of heat is determined by the difference between the incoming solar radiation and the outgoing back radiation, conduction and loss due to evaporation.

A steady state balance for a given Q_{net} for natural sources and sinks of heat is established as a control case with no reactor cooling water intake. Then, as various intake-outlet configurations are tested, $Q_{\Delta T}$ is found by using the net heat balance for an overtemperature (Milanov, 1969). The net heat loss due to the overtemperature can be obtained from the relation,

$$Q_{\Delta T} = \frac{\partial Q_{\Delta T}}{\partial T} \Delta T = \left(\frac{\partial Q_b}{\partial T} + \frac{\partial Q_c}{\partial T} + \frac{\partial Q_e}{\partial T}\right) \Delta T \tag{3.23}$$

where ΔT is the overtemperature

$Q_{\Delta T}$ is the net loss due to the overtemperature

Q_b is the loss due to back radiation

Q_c is the loss due to conduction to the atmosphere

Q_e is the loss due to evaporation

The relation for the back radiation as a function of temperature, is,

$$\frac{\partial Q_b}{\partial T} = 8.26 \cdot 10^{-11} \cdot 0.97 \cdot 4(273 + T)^3 \tag{3.24}$$

It is independent of wind velocity. The loss due to conduction is,

$$\frac{\partial Q_c}{\partial T} = 0.00534(1.0 + 0.6\, u_{wind}) \tag{3.25}$$

where u_{wind} is the wind velocity in meter/second at 15 meters height. It is independent of the temperature. The loss due to evaporation is,

$$\frac{\partial Q_e}{\partial T} = (1.0 + 0.6\, u_{wind}) \frac{42.167}{(235 + T)^2} E_o \cdot 10^{\left(\frac{7.45\, T}{235 + T}\right)} \tag{3.26}$$

where E_o is the vapor pressure at 0^oC. The units for $\frac{\partial Q}{\partial T}$ are cal cm^{-2} min^{-1} $degree^{-1}$.

It has been found (Milanov 1969) that only about 10 % of the temperature reduction in the near field zone at certain existing heated water discharge points can be accounted for by loss to the atmosphere. The rest is due to mixing with the ambient water and advection out of the region. This model cannot hope to accurately represent the atmospheric losses in the near field zone. The scale of the near field is on the order of 1 kilometer which is the horizontal grid spacing. The representation here approximates the near field by mixing the heat over one grid volume (about 10^6 m^3). Atmospheric losses represent an effective control on extreme overtemperatures at the surface but do not reduce the heat content of the water significantly.

At a surface intake point there is an additional heat loss due to the advective flux into the intake. The net flux at the surface is due to the natural net radiation, atmospheric losses due to overtemperature and intake into the cooling system:

$$\text{Net flux} = + wT - K_v^T \frac{\partial T}{\partial z} = \frac{Q_{net}}{\rho_o C_P} - \frac{Q_{\Delta T}}{\rho_o C_P} + (wT)_{intake} \qquad (3.27)$$

At an outlet point the net flux is due to the natural net radiation, atmospheric losses due to overtemperature, heat transported from the intake and heat added by the condenser stage of the reactor cooling system:

$$\text{Net flux} = + wT - K_v^T \frac{\partial T}{\partial z} = \frac{Q_{net}}{\rho_o C_P} - \frac{Q_{\Delta T}}{\rho_o C_P} + |wT|_{intake} + \frac{Q_{reactor}}{\rho_o C_P} \qquad (3.28)$$

The boundary conditions at the oceanic side is similar to the one expressed for salinity:

$$\begin{aligned} T &= T_o(z, t), \quad u \leq 0 \\ \frac{\partial T}{\partial x} &= 0, \qquad u > 0 \end{aligned} \qquad (3.29)$$

The predictive equation for temperature states that the time change of temperature is due to advection and turbulent diffusion.

The sources of heat are net solar radiation and heated reactor cooling water from the outlet. Both are at the surface and represent an excess buoyancy which tends to stably stratify the water. In addition, there are losses due to an overtemperature. A destabilizing effect can occur when bottom intake water is discharged into surrounding water of a higher temperature (summer conditions).

3.7 Equation of State

The equation of state for sea water expresses the relation between density and temperature, salinity and pressure. In a shallow estuary pressure effects can be ignored and the density can be represented as,

$$\rho = \rho_o(1 + \sigma_t \, 10^{-3}) \tag{3.30}$$

where σ_t is defined from Knudsen's Hydrographical Tables, (1901).

The following relations define $\sigma_t(S, T)$

$$\Sigma_T = - \frac{(T - 3.98)^2}{503.570} \cdot \frac{(T + 283)}{(T + 67.26)}$$

$$Cl = \frac{S - 0.030}{1.8050}$$

$$\sigma_o = -0.069 + 1.4708Cl - 0.001570Cl^2 + 0.0000398Cl^3$$

$$A_T = T(4.7867 - 0.098185T + 0.0010843T^2) \cdot 10^{-3}$$

$$B_T = T(18.030 - 0.8164T + 0.01667T^2) \cdot 10^{-6}$$

$$\sigma_t = \Sigma_T + (\sigma_o + 0.1324)(1 - A_T + B_T(\sigma_o - 0.1324)) \tag{3.31}$$

3.8 Scaling

The dimensional variables can be replaced by products of a scale and a non-dimensional variable,

$$\begin{aligned}
t &\to t_o \cdot t' \\
x &\to L \cdot x' \\
z &\to H \cdot z' \\
u &= U \cdot u' \\
w &= \frac{U \cdot H}{L} \cdot w' = W \cdot w' \\
S &= S_o \cdot S' \\
T &= T_o \cdot T' \\
b &= B \cdot b' \\
\eta &= \frac{U}{H} \cdot \eta' \\
Q &= \rho_o C_P W T_o \cdot Q' \\
\tau &= \frac{A_v \rho_o U}{H} \cdot \tau'
\end{aligned} \tag{3.32}$$

The time scale, t_o, is determined by the advection time

$$t_o = \frac{L}{U} \tag{3.33}$$

The eddy diffusivities and viscosities have been taken as constants for this study and will appear in non-dimensional constants.

3.9 Non-dimensional Equations

The non-dimensional salt equation is (dropping the '),

$$b \frac{\partial S}{\partial t} + \frac{\partial}{\partial x}(ubS) + \frac{\partial}{\partial z}(wbS) = \varepsilon \frac{\partial}{\partial z}(b \frac{\partial S}{\partial z}) + \varepsilon\delta \frac{\partial}{\partial x}(b \frac{\partial S}{\partial x}) \tag{3.34}$$

where $\varepsilon = \frac{K_v^S}{H \cdot W}$ = ratio of the advective time scale to the diffusive time scale.

$\delta = \frac{K_h^S H^2}{K_v^S \cdot L^2}$ = ratio of the horizontal mixing to the vertical mixing.

The non-dimensional boundary conditions are the same as before except for (3.16) which becomes,

$$wS = \varepsilon \frac{\partial S}{\partial z}, \quad z = 0$$

The heat equation is derived in a similar way,

$$b \frac{\partial T}{\partial t} + \frac{\partial}{\partial x}(ubT) + \frac{\partial}{\partial z}(wbT) = \varepsilon \frac{\partial}{\partial z}(b \frac{\partial T}{\partial z}) + \varepsilon\delta \frac{\partial}{\partial x}(b \frac{\partial S}{\partial x}) \tag{3.35}$$

where the non-dimensional numbers are the same as before. This implies that salt and heat diffuse in the same way. It is not possible to go further with the mixing assumptions until more experimental work is performed in Bråviken. The surface heat condition without an intake becomes in non-dimensional form,

$$\text{Net flux} = + wT - \varepsilon \frac{\partial T}{\partial z} = Q_{net} \tag{3.36}$$

With an intake, the surface boundary condition for heat becomes,

$$\text{Net flux} = + wT - \varepsilon \frac{\partial T}{\partial z} = Q_{net} - Q_{\Delta T} \tag{3.37}$$

except at the intake point where it is

$$\text{Net flux} = +wT - \varepsilon \frac{\partial T}{\partial z} = Q_{net} - Q_{\Delta T} + (wT)_{intake} \tag{3.38}$$

and at the outlet where it becomes

$$\text{Net flux} = +wT - \varepsilon \frac{\partial T}{\partial z} = Q_{net} - Q_{\Delta T} + |wT|_{intake} + Q_{reactor} \tag{3.39}$$

The non-dimensional vorticity equation is

$$\frac{\partial \eta}{\partial t} + u \frac{\partial \eta}{\partial x} + w \frac{\partial \eta}{\partial z} = Pr\varepsilon \left(\frac{\partial^2 \eta}{\partial z^2} + \delta \frac{\partial^2 \eta}{\partial x^2}\right) + \varepsilon^2 PrRa \frac{\partial \sigma_T}{\partial x} \tag{3.40}$$

where Pr = the turbulent Prandtl number = the ratio of the viscosity to the eddy diffusivity (of salt or heat) = A_v/K_v, Ra = the estuarine Rayleigh number = $\frac{g \cdot H^5 \cdot \sigma_s}{K_v \cdot A_v \cdot L^2}$ where σ_s is the σ_t scale factor 10^{-3}.

The product of $\varepsilon^2 PrRa$ is the inverse internal Froude number,

$$\varepsilon^2 PrRa = \frac{g \cdot \sigma_s \cdot H}{U^2} = Fr^{-1} \tag{3.41}$$

and is the ratio of the advective time scale to the internal vorticity generation time scale. The vorticity boundary conditions in non-dimensional form are,

$$\eta = \tau_w \quad z = 0 \text{ at the surface and}$$
$$\eta = \tau_b \quad z = h \text{ at the bottom} \tag{3.42}$$

4. NUMERICAL METHOD

4.1 The Grid

The set of non-dimensional equations and their boundary conditions is a predictive system and can be numerically integrated in time from a known initial field. The variables are defined on a grid and finite difference approximations to the equations are written. The grid used consists of two staggered grids, one on which salinity and temperature are defined and the other on which vorticity and streamfunction are defined (Figure 4.1). The boundary is defined by the streamfunction grid. The sum and difference operators adopted by Shuman (1962),

$$S_x \equiv \frac{1}{\Delta x}\left(S(x_i + \frac{\Delta x}{2}) - S(x_i - \frac{\Delta x}{2})\right) \qquad (4.1)$$

$$\bar{S}^x \equiv \frac{1}{2}\left(S(x_i + \frac{\Delta x}{2}) + S(x_i - \frac{\Delta x}{2})\right) \qquad (4.2)$$

will be used here. A superscript n denotes the time level.

4.2 Time Differencing

The time differencing scheme chosen is the leapfrog. That is, the prediction at the n + 1 level is explicitly determined from evaluation of the variable at the n - 1 level, the advection and density driving terms at the n time level and the diffusion terms at the n - 1 level. For example, the vorticity equation has the following time structure,

$$\frac{\eta^{n+1} - \eta^{n-1}}{2\Delta t} = -(\text{advection of } \eta)^n + (\text{diffusion of } \eta)^{n-1}$$

$$+ (\text{density generation of } \eta)^n \qquad (4.3)$$

Many explicit and implicit schemes have been investigated (for example Grammeltvedt, 1969, Young, 1968, Fisher, 1965, Kurihara, 1965, et. al.) for the prediction equations with non-linear terms, but the leapfrog is still considered the most accurate and efficient. A computational mode results since the leapfrog is defined on three time levels. In the absence of sufficient friction, the computational mode grows and eventually causes splitting of the solution at adjacent time steps. This can be suppressed by smoothing or restarting at regular time intervals, without loss of accuracy or speed. A scheme such as the leapfrog-trapezoidal in which the computational mode is completely removed requires twice as much computation time as the leapfrog with periodic smoothing. Other schemes, such as two step schemes or implicit schemes, usually have undesirable artificial damping of the physical solution.

There is a maximum time step for numerical stability of leapfrog advection and lag diffusion. The Courant-Friedrichs-Lewy number is defined as

$$CFL = \Delta t \left((\frac{U}{\Delta x})_{max} + (\frac{W}{\Delta z})_{max} \right) \tag{4.4}$$

and the critical CFL number can be written as

$$CFL\ CRITICAL = (1 - 8\Delta t \left(\frac{A_v}{\Delta z^2} + \frac{A_h}{\Delta x^2} \right))^{1/2} \tag{4.5}$$

The stability criteria (Ogura and Yagihashi, 1969) is that the maximum time step, Δt, must satisfy the relation

$$CFL < CFL\ CRITICAL \tag{4.6}$$

4.3 Finite Difference for Diffusion

The salt diffusion term is written as

$$\varepsilon \left((\bar{b}^z S_z)_z + \delta (\bar{b}^x S_x)_x \right)^{n-1} \tag{4.7}$$

and the heat diffusion term similarily as

$$\varepsilon \left((\bar{b}^z T_z)_z + \delta (\bar{b}^x T_x)_x \right)^{n-1} \tag{4.8}$$

The correct no diffusive salt or heat flux boundary condition, which holds on the bottom and on the oceanic boundary for outflowing water, is

$$T_z^{n-1} = 0,\ S_z^{n-1} = 0 \qquad \text{on horizontal boundaries} \tag{4.9}$$

and

$$T_x^{n-1} = 0,\ S_x^{n-1} = 0 \qquad \text{on vertical boundaries} \tag{4.10}$$

The vorticity diffusion takes the form

$$Pr\varepsilon \left((\eta_z)_z + \delta (\eta_x)_x \right)^{n-1} \tag{4.11}$$

The oceanic boundary condition is given as

$$\eta_x^{n-1} = 0 \tag{4.12}$$

4.4 Finite Difference for Advection

The advection of salt and heat is written in the flux form (Arakawa, 1966) in order to conserve the mean and variance of salt and heat. This method is correct as long as continuity is satisfied at every grid point (Piacsek and Williams, 1970). Continuity for the grid chosen is identically satisfied everywhere:

$$(\Psi_x)_z + (-\Psi_z)_x = 0 \tag{4.13}$$

The velocity is defined at the midpoint between two salinity or heat points so that the flux form is

$$\left[(bu\bar{S}^x)_x + (bw\bar{S}^z)_z\right]^n \tag{4.14}$$

and

$$\left[(bu\bar{T}^x)_x + (bw\bar{T}^z)_z\right]^n \tag{4.15}$$

This form of advection prevents non linear instability due to aliasing on the grid (Lilly, 1965). The bottom boundary condition requiring no advective flux in the absence of an intake is identically satisfied by the above equation. The bottom intake boundary condition is satisfied by the above equation in combination with (4.9).

The advection of vorticity is expressed in the Arakawa form which conserves vorticity and kinetic energy,

$$\frac{1}{b}\left[(\eta(-\bar{\Psi}^z)_z)_x + (\eta(\bar{\Psi}^x)_x)_z\right] \tag{4.16}$$

The boundary conditions take the same form as the continuous equations.

4.5 Advective-Diffusive Salt and Heat Surface Boundary Conditions

The surface boundary conditions for salt and heat contain both advective and diffusive fluxes. These boundary conditions must be consistent with the interior equations. The surface boundary conditions on salt and heat, away from the intake and outlet, are respectively,

$$(w\bar{S}^z)^n = \varepsilon S_z^{n-1} \tag{4.17}$$

and

$$-\varepsilon T_z^{n-1} + (w\bar{T}^z)^n = Q_{net} - Q_{\Delta T} \tag{4.18}$$

At the intake point the net salt flux,

$$-(\varepsilon S_z^{n-1})_{intake} + (w\bar{S}^z)^n_{intake} = +(w\bar{S}^z)^n_{intake} \qquad (4.19)$$

that is, $(\varepsilon S_z^{n-1})_{intake} = 0$

at a surface intake point.

At the surface intake point the net heat flux

$$\left[-(\varepsilon T_z^{n-1})_{intake} + (w\bar{T}^z)^n_{intake}\right] = +(w\bar{T}^z)^n_{intake} + Q_{net} - Q_{\Delta T}$$

or

$$-(\varepsilon T_z^{n-1})_{intake} = Q_{net} - Q_{\Delta T} \qquad (4.20)$$

At an outlet point the net salt flux is due to the salt advected through the cooling system,

$$\left[-(\varepsilon S_z^{n-1}) + (w\bar{S}^z)^n\right]_{outlet} = +\left|(w\bar{S}^z)^n_{intake}\right| \qquad (4.21)$$

At the outlet point the net heat flux is,

$$\left[-(\varepsilon T_z^{n-1}) + (w\bar{T}^z)^n\right]_{outlet} = +\left|(w\bar{T}^z)^n_{intake}\right| + Q_{net} - Q_{\Delta T} + Q_{reactor} \qquad (4.22)$$

4.6 Finite Difference for the Streamfunction

After each prediction of the salinity, temperature and vorticity is made, the streamfunction is obtained by integrating the finite difference equation,

$$\eta = \left(\frac{\Psi_z}{\bar{b}^z}\right)_z \qquad (4.23)$$

from $z = h(x)$ to $z = 0$. Then $\Psi_{bc}(z)$ is added to the streamfunction to satisfy the surface and bottom boundary conditions

$$\Psi = \Psi_B, \quad z = h \qquad (4.24)$$

$$\Psi = \Psi_S, \quad z = 0 \qquad (4.25)$$

The function Ψ_{bc} at the surface and bottom is the correction to the solution of (4.23) necessary to satisfy (4.24) and (4.25). The function Ψ_{bc} satisfies the equation,

$$\left[\frac{(\Psi_{bc})_z}{\bar{b}^z} \right]_z = 0 \qquad (4.26)$$

4.7 Equation of State

In order to simplify numerical computation for the density, several approximations to σ_T have been found. The one chosen for use here is shown in Figure 4.6 compared with σ_T. The approximation to Knudsen's is,

$$\sigma_T(T, S) = -0.072169 + (T - 0.5)(0.049762 + (T - 0.5)$$
$$(-0.0075911 + 0.000035187\ (T - 0.5))) + S(0.80560 +$$
$$+ (T - 0.5)(-0.0030063 + 0.000037297(T - 0.5))) \qquad (4.27)$$

The form was adapted from Fredrich and Levitus (1972). The original approximation was developed for high salinity, 35 o/oo, oceanic models. It was found that by shifting the temperature by $0.5^{o}C$ a better fit occured at low salinities. It requires only about one third the computational time of the full σ_t relation.

4.8 The Numerical Procedure

The procedure to obtain the solution as a function of time can be summarized as follows:

1) initialization of the fields and parameters

2) time stepping of the salinity equation and application of boundary conditions (Figure 4.2)

3) time stepping of the temperature equation and application of boundary conditions (Figure 4.3)

4) time stepping of the vorticity equation and application of boundary conditions (Figure 4.4)

5) computation of the streamfunction with proper boundary conditions imposed (Figure 4.5)

6) periodic suppression of the computational mode and computation of the averages and variances for output

7) periodic storage of data for later graphical display

8) return to 2) until the computation is complete

Since steps 2), 3) and 4) are not dependent on knowing other variables on the n + 1 level,

$$(S, T, \eta)^{n+1} = f(S, T, \eta)^{n,\ n-1}$$

they may occur in any order.

5. RESULTS

5.1 Philosophy of the Model

The basic questions to be answered are: what effect does the excess buoyancy have on the circulation of the estuary and how large an excess temperature can be expected in various parts of the estuary under reasonable conditions. A numerical model is used to represent the interaction between waste heat and the estuarine circulation. It is a controlled experiment. The control is the numerical simulation of the natural state of Bråviken. The heated water simulation is added to the control to predict the conditions to be expected in Bråviken after construction of the reactor. The results of these simulations are compared to the control in order to evaluate the impact of the plant. This is not a comparison with the real natural state but with a model of the natural state. In the future a field program should be carried out to validate the model of the natural state.

The natural conditions modelled represent two states of thermal stratification: summer with a strong vertical temperature gradient and winter with essentially no vertical temperature variation. These two states are established by imposing typical conditions on the net surface heat flux.

For each of these seasons, two different intake configurations have been considered: a surface intake, as is planned, and a bottom intake. In all cases the outlet is located at the surface and on the oceanic side of the intake. Several typical wind conditions have been considered: no wind, a steady wind of 5 m/s and a 12 m/s time dependent wind which gradually builds from the west, shifts to the east and then dies. A series of experiments, under the winter conditions and with varying degrees of runoff, has also been conducted.

5.2 Scales and Parameters

The computations were carried out on a CDC 6600 computer. Computations at one time step on the 47 x 52 grid required about 0,4 seconds of computer time. One time step represents about 1 000 seconds of realtime. The values of parameters were chosen so that the simulation of the natural state was an accurate representation of the field measurements taken during August 1973 and November 1973. There were no additional data available at the outset of the computations to permit further calibration of the model. There were no direct measurements of the critical parameters: eddy viscosity and diffusivity. The following values were found to give equally good comparisons with both the winter (November) and summer (August) measurements:

$K_v = 5\ cm^2/s = A_v$

$K_x = 5 \times 10^6\ cm^2/s = A_x$

The other scales chosen were,

$U \approx 10$ cm/s $\quad B \approx 10^5$ cm

$H \approx 10^3$ cm $\quad T \approx 10^{o}C$

$L \approx 10^6$ cm $\quad S \approx 10$ o/oo

The remaining scales were obtained from those above,

$$W = \frac{U}{L} H = 10^{-2} \text{ cm/s}$$

$$\Psi = U \cdot B \cdot H = 10^9 \text{ cm}^3/\text{s}$$

$$Q = W \cdot T \cdot \rho_o \cdot C_P = 10^{-1} \frac{\text{gcal}}{\text{cm}^2 \cdot \text{s}}$$

$$\eta = \frac{U}{H} = 10^{-2} \text{ 1/s}$$

$$t_o = \frac{L}{U} = 10^5 \text{s}$$

The non-dimensional parameters are found to be,

$\varepsilon = 0.5$

$\delta = 1.0$

$Pr = 1.0$

$Fr = 10.0$

The solutions given are non-dimensional unless otherwise stated. The dimensional values can be obtained by multiplying by the proper scale above. The fields of temperature, salt and vorticity are non-dimensional.

A vector flux of each quantity is shown as well. The fluxes are defined as follows:

$$\text{Salt flux} = \rho_o \Big[S \cdot \Big(\underbrace{\Big(-\frac{\partial \Psi}{\partial z}\Big) \vec{i} + \Big(+\frac{\partial \Psi}{\partial x}\Big) \vec{k}}_{\text{Advective Salt Flux}} \Big)$$

$$\underbrace{- \varepsilon' \Big(\delta b \frac{\partial S}{\partial x} \vec{i} + b \frac{\partial S}{\partial z} \vec{k} \Big)}_{\text{Diffusive Salt Flux}} \Big]$$

$$\text{Heat flux} = \rho_o C_P \left[T\left(\left(-\frac{\partial \Psi}{\partial z}\right)\vec{i} + \left(+\frac{\partial \Psi}{\partial x}\right)\vec{k}\right)\right.$$

Advective Temperature Flux

$$\left. - \varepsilon \left(\delta b \frac{\partial T}{\partial x}\vec{i} + b\frac{\partial S}{\partial z}\vec{k}\right)\right]$$

Diffusive Temperature Flux

$$\text{Vorticity flux} = \eta\,(u\vec{i} + w\vec{k}) - Pr \cdot \varepsilon\left(\delta \frac{\partial \eta}{\partial x}\vec{i} + \frac{\partial \eta}{\partial z}\vec{k}\right)$$

Advective Vorticity Flux — Diffusive Vorticity Flux

where $\vec{i}$, $\vec{k}$ are the unit vectors in the x, z directions. The salt and temperature conservation equations state that the divergence of the salt and temperature is the rate of change of salinity and temperature. So, for a steady state, the salt and temperature fluxes are non-divergent. The vorticity equation cannot be stated as simply because it represents a balance at the center of the channel and not a flux integrated across the channel. The advection and diffusion have been represented as a flux to illustrate the relative importance of advection or diffusion of vorticity. In a channel of constant width, the vorticity equation can be represented in a form analogous to the salt and temperature equations. In general, the advection dominates the salt and temperature fields while advection and diffusion are of equal importance in the vorticity field. The scales of the fluxes are,

$$\text{Salt flux} = S\,\frac{g}{1000g} \cdot U \cdot B \cdot \rho_o = 10^4\,\frac{g}{s \cdot cm}$$

$$\text{Heat flux} = C_P \cdot T \cdot U \cdot B \cdot \rho_o = 10^7\,\frac{cal}{s \cdot cm}$$

$$\text{Vorticity flux} = \frac{U}{H} \cdot U = 10^2\,\frac{cm}{s^2}$$

5.3 Summer: Natural Conditions

The natural summer temperature and salinity fields are shown in Figures 5.1 and 5.2. These sections were taken during 1973, a year when the runoff was relatively low. The experiments were conducted with the runoff at 50 m^3/s, an average value for 1973. The other boundary conditions were established from separate hydrographic casts taken at the same time (Figure 2.6). The salinity of the Baltic was set at a constant 7 o/oo. The temperature of the Baltic source water was set at 5^oC. These values correspond well with the temperature and salinity values below about 30 meters obtained from the sections (Figure 5.1 and 5.2).

The computer simulation of the natural summer conditions was obtained using a net solar flux of about 10^{-3} cal/cm^{2}sec and a river heat flux of about the same magnitude. The resulting isotherms (Figure 5.3 and 5.6) correspond quite well with those of the measurements (Figure 5.1). The surface temperature is about 19.6°C and the bottom temperature inside the sill is about 10°C.

The salinity (Figure 5.4) obtained compares quite well with the observed field (Figure 5.2). There were no measurements of velocity available with which to obtain a vorticity comparison (Figure 5.5).

5.4 Summer: Surface and Bottom Intake with No Wind

A surface intake and outlet have been added to the simulated natural conditions. A volume flux through the reactor cooling system, of 300 m^3 /sec, has been used for all intake-outlet simulations. This is the proposed capacity of the cooling system at Tunaberg. The water is heated 10°C. The net flux of heat out of the reactor cooling system is about 12 500 MW. The temperature field shows that the natural isotherms are deeper than before (Figure 5.7 and 5.10) and that there is a heated water plume at the outlet. The salinity in Bråviken is shown (Figure 5.8) to decrease slightly indicating a restriction (Figure 5.9) in the inflow of salty Baltic water.

With a bottom intake the surface temperature at the outlet is decreased (Figure 5.11 and 5.14). The salinity (Figure 5.12) has increased slightly above that for the simulated natural conditions indicating a very slightly enhanced estuarine flow (Figure 5.13).

5.5 Summer: Surface and Bottom Intake with a Time Dependent Wind

An experiment was conducted with a time dependent wind whose maximum was about 12 m/s. It was imposed as a sinusoid with a period of six days followed by fourteen days of no wind (Figure 5.19). The wind blew from the west for the first three days and then from the east for the next three. This meant that the flow was out of Bråviken for the first three days and into Bråviken for the next three days.

The results are shown at a time fourteen days after the wind has stopped. With a surface intake the surface temperature and plume temperature are much higher (Figure 5.15 and 5.18) than with no wind or in the natural case. During the period of time in which the wind drives heat into Bråviken, the temperature rises rapidly (Figure 5.19). The recovery of Bråviken is quite slow after this because the runoff transport is so much smaller than the wind transport which trapped the heat in Bråviken. The wind transport is typically 10 to 20 times the runoff of 50 m^3/s. As before, the salinity decreases slightly (Figure 5.16) due to a decrease in the estuarine flow (Figure 5.17). Vertical profiles reveal the influence of the disturbance on the density and velocity field (Figure 20). The surface temperature is seen to increase by about 3°C(Figure 20 a, b, c). The salinity returns to almost the same

values as before the storm (Figure 20 d, e, f). The flow remains reduced in the upper five meters (Figure 20 g, h, i). The strong vertical shear in the flow due to the wind can be seen in the velocity profile. With a bottom intake the wind disturbance has little effect on Bråviken. The temperature field after fourteen days (Figure 5.21 and 5.24) is virtually the same as before with the bottom intake and no wind (Figure 5.11). There has been a slight inflow of salt at depth (Figure 5.22). The flow is as before (Figure 5.23). The time curves for the mean values (Figure 5.25) show that the effects of the disturbance pass quickly.

The vertical profiles (Figure 26) reveal that the temperature, salinity and velocity all return to normal quite rapidly. The range of surface temperatures (Figure 26 a, b, c) during the wind event is about as great as with a surface intake but the maximum is less and the recovery faster. The salinity range due to the wind transport is much the same with a bottom intake as with a surface intake. The surface salinity (Figure 26 d, e, f) is higher with the bottom intake due to the outlet of high salinity bottom water at the surface. The velocity at the surface (Figure 5.26 g, h, i) is not as restricted as with a surface intake and promotes the rapid flux of excess heat out of Bråviken.

5.6 Comparison of the Summer Cases

The vertical temperature, salinity and velocity for the five summer cases investigated have been plotted (Figure 5.27) for comparison. The profiles for the time dependent winds have been plotted for a time fourteen days after the wind ceases. It is clear that the vertical temperature distribution is only affected by a surface intake (Figure 5.27 a, b, c). The temperature rise at the outlet is about 3° higher with no wind than the natural state and about 9° higher fourteen days after a strong wind system has passed through the region.

The salinity of the upper 20 meters is increased due to the bottom intake (Figure 5.27 d, e, f). The cooling system removes bottom water of a higher salinity than the surface water and returns it to the surface. The salinity with a surface intake is reduced. This is due to the buoyant heated water plume restricting the natural supply of salt from the Baltic.

The estuarine circulation (Figure 5.27 g, h, i) is increased slightly by the bottom intake in the summer. However, the natural flow is severly restricted by a surface intake.

The surface intake creates a severe thermal stress and has an adverse effect on the natural estuarine circulation in Bråviken during the summer. The bottom intake produces no noticable thermal stress and slightly enhances the natural circulation. The enhanced circulation would increase oxygen renewal in the deep waters of Bråviken and generally have a beneficial effect on the estuary.

5.7 Winter: Natural Conditions

The natural winter temperature and salinity fields (Figure 5.28 and 5.29) show a reasonable correspondence to the same boundary conditions established for the summer. The major difference

between the winter and summer sections are:

the lack of vertical temperature stratification in the winter, and

a smaller salt dilution in the winter.

The simulation of natural winter conditions was established using a runoff of 50 m^3/s and no net surface heat flux. Later in the winter a net loss occurs resulting in surface temperatures of 2°C. However, no sections were available for this part of the year for comparison. The temperature field (Figure 5.30, 5.33) was almost isothermal at 5°C. The salinity field (Figure 5.31) compares well when it is remembered that the source salinity used as a boundary condition was a bit lower than that found from the section. The boundary conditions for the summer and winter cases were set to the same values in order to evaluate the effect of solar heating on the estuarine circulation. By comparing the salt fluxes in the summer (Figure 5.4) and winter (Figure 5.31) it can be seen that the estuarine circulation is slightly greater in the summer due to natural longitudinal temperature gradients. This is difficult to establish from the salinity data (Figures 5.2 and 5.29) alone. The region of greater dilution in the summer is due to the reduction of vertical mixing due to thermal stratification. This model studies only constant vertical mixing.

The vorticity (Figure 5.5) in the summer is larger than in the winter (Figure 5.32). This is a direct measure of the increased estuarine circulation in the summer.

5.8 Winter: Surface and Bottom Intake with No Wind

A surface intake and outlet have been added to the simulated natural winter conditions. The reactor heating is as before for the summer case. The temperature field (Figure 5.34 and 5.37) with surface intake shows a rather extensive heated water plume. As before, the heated water restricts the estuarine circulation (Figure 5.36) which causes an increased dilution of salt water (Figure 5.35). The effect of the surface intake is more obvious and pronounced in the winter than in the summer, due to the slower natural flow out of Bråviken at the surface.

The bottom intake provides little relief from the heated water plume. The temperature (Figures 5.38 and 5.41) is qualitatively the same and only slightly less in magnitude than with the surface intake. The salinity (Figure 5.39) is higher than with the surface intake. The cooling system with a bottom intake pumps salty bottom water to the surface. The circulation (Figure 5.40) is not restricted as much as with the surface intake but the restriction is still considerable.

5.9 Winter: Surface and Bottom Intake with a Time Dependent Wind

The same time dependent wind that was used in the summer case was applied to the winter simulation; a 12 m/s wind blowing from the west three days which then shifts to the east for three days before dying out. Fourteen days after the wind has stopped the

surface intake has produced (Figures 5.42, 5.45) an enlarged plume due to the trapping of heated water in Bråviken. The wind transports that trap the heat are of an order of magnitude greater than the estuarine circulation which tries to advect the heat out into the Baltic. The result is that it takes longer, by an order of magnitude, for the natural circulation to flush out Bråviken than it took for the wind to drive up the temperature (Figure 5.46). The higher wind induced surface temperature restricts the flow (Figure 5.44) and increases the salinity (Figure 5.43) over the levels obtained without wind.

The vertical profiles (Figure 5.47) in time illustrate the slow recovery of Bråviken from a wind disturbance. The temperature difference at the surface is almost one degree (Figure 5.47 a, b, c). The salinity profiles (Figure 5.47 d, e, f) show a faster recovery than was seen with heat because there are no salt sources to compare with the reactor heat source. The velocity profiles are dominated by the wind currents (Figure 5.47 g, h, i).

The results obtained with a bottom intake in the winter with a time dependent wind are much the same as those obtained with a surface intake. The temperature plume (Figure 5.48 and 5.51) is not as extensive as with the surface intake but is larger than the plume obtained under conditions of no wind and with the bottom intake. The reasons are the same as those with the surface intake. The salinity (Figure 5.49) is much the same as without wind (Figure 5.39). The circulation (Figure 5.50) is slightly greater than with no wind. The recovery time is much faster (Figure 5.52) with a bottom intake than with a surface intake. The bottom intake removes the effects of recirculation through the heating system. It does not prevent wind trapping of the surface plume, however. The vertical profiles (Figure 5.53) show lower temperature levels obtained (Figure 5.53 a, b, c) with the bottom intake as opposed the surface intake (Figure 5.47 a, b, c) and a wind. The salinities with the bottom intake are generally higher (Figure 5.53 d, e, f) than the salinities with a surface intake (Figure 5.47 d, e, f) although the range during a wind event is about the same. The wind driven velocities dominate again (Figure 5.53 g, h, i).

5.10 Comparison of the Winter Cases

The vertical temperature, salinity and horizontal velocity for the five winter cases investigated have been plotted (Figure 5.54) for comparison. The profiles for the time dependent winds have been plotted for a time fourteen days after the wind ceases. The temperature increases in all cases over that in the natural state. The surface intake with and without wind causes the greatest temperature rise (Figure 5.54 a, b, c).

The salinity is decreased most by the surface intake with and without wind (Figure 5.54 d, e). At the outlet there is a slight salinity increase due to the bottom intake (Figure 5.54 f).

The estuarine circulation is restricted in all winter cases (Figure 5.54 g, h, i). The greatest reduction of the natural flow is by the surface intake. The circulation can be reduced to almost nothing.

Adverse affect on the circulation and possibilities of thermal stress in the winter occur for both the surface and bottom intakes. The bottom intake has a somewhat smaller effect than the surface intake.

5.11 Surface Intake in the Winter for Various Runoffs

During the winter season thermal stresses as well as restriction in natural flow are likely to occur even with a bottom intake. It is of interest to investigate what effect a stronger natural flow would have on the overtemperature under the most severe conditions, surface intake in the winter. This is the same as considering a reactor with a much smaller cooling system. The important measure here is the ratio of the runoff to the cooling water transport. The estuarine circulation is more or less proportional to the runoff. As runoff increases, dilution of salt increases and the horizontal density gradient increases. This, in turn, drives a stronger estuarine flow, permitting a more rapid transport of heat out of Bråviken.

A series of experiments with runoffs of 50, 100, 150, 200, 250 and 300 m^3/s were run without an intake as a control (Figures 5.55, 5.56, 5.57). As the runoff increases, the temperature in the shallowest parts decreases (Figure 5.55) due to a slight river cooling. The salt dilution (Figure 5.56) increases rapidly with runoff. As the dilution increases, so does the vorticity, or the estuarine circulation (Figure 5.57). The vertical profiles further illustrate this behavior (Figure 5.58). The estuarine circulation increases about 2.5 times for an increase in runoff of about 6 times (Figure 5.58 g, h, i).

A surface intake was added and compared with the control. In order to isolate the effect of the increased advective transport of heat out of Bråviken due to increased runoff, losses to the atmosphere were ignored. In all previous reactor cases, losses to the atmosphere were considered. A comparison of Figure 5.59 a, in which there were no losses, with Figure 5.34, with losses and the same runoff, shows the effect of atmospheric losses on the overtemperature. As the runoff increases the plume decreases (Figure 5.59 a, b, c, d, e, f). The salinity with an intake is generally lower than without (Figure 5.56 a, b, c, d, e, f; Figure 5.60 a, b, c, d, e, f).

However, the increased dilution due to increased runoff is about the same with and without the intake. The vorticity (Figure 5.61 a, b, c, d, e, f) for a large runoff and a surface intake approaches the values obtained with no intake. The vertical profiles (Figure 5.62 a, b, c, d, e, f, g, h, i) further illustrate that increased runoff removes much of the influence of the heated cooling water.

5.12 Comparison of Results with Field Measurements

As a part of the study of Bråviken as the possible site for a nuclear power plant, hydrographic measurements were made. Most of the measurements were made in the region near the planned outlet. No measurements were made at the sill of Brå-

viken. There were two stations at Lönö, a few kilometers outside the sill. There exist two channels at Lönö.

Estimates of the volume transport have been made (E Bergstrand, personal communication) from these measurements, Table 5.1. There is a general correlation between wind and transport. However, when all data are averaged it is impossible to determine the runoff with any certainty. For a typical numerical experiment with a time dependent wind, the maximum transport in at the bottom is about 1 300 m^3/sec. The transport out at the surface is this plus the runoff. The observed transport during strong winds was of this order of magnitude.

Some vertical profiles of measured velocity are included to show that the magnitude and curvature of the velocity sections agree with the numerical experiment. These profiles (Figure 5.63) can be compared with any of the numerical profiles for a time dependent wind. It has not been possible to compare temperature and salt profiles. What is important to compare in so far as salt and heat are concerned, are the changes during variable wind conditions and not the mean profile. However, data in time were too incomplete to make this comparison.

Because the measurements available to date are too incomplete to make detailed comparisons with the numerical data, a field program, designed to measure water, salt and heat transports as a function of changing external conditions, is necessary to properly calibrate the model.

In comparing the profiles of heat and salt from data with the numerical experiments one feature is lacking in the numerical results. The sharpness of the real halocline-thermocline is not well represented. This is due to the fact that a constant eddy mixing has been used. Further model development has taken place to include mixing dependent on stratification. The results compare favorably with the natural pycnocline. It is not likely that this new development will alter any of the qualitative results presented here.

Table 5.1
Transport values calculated from weekly current measurements at two stations in the mouth of Bråviken (positive transport is out of the bay)

Date	Transport, m^3/s		Wind at 10 m above sea level, m/s
	Above main pycnocline	Below main pycnocline	
1974-04-03	-1023	+1648	E 4
04-10	+664	-373	W 4
04-17	+518	+146	NW 2
04-24	-920	+552	NE 2
05-01	-958	+463	NE 10
05-08	+727	-619	NW 11
05-15	+533	-752	N 10
05-21	-1083	+1493	SE 8
05-29	+767	-1273	SSW 5
06-05	+1919	+834	W 9
06-12	-540	-202	NNE 10
06-19	+156	-153	W 2
06-26	-944	+194	SE 9
07-04	+1131	-1297	W 2
07-10	+888	-395	NE 1
07-17	+374	-219	SE 2
07-24	+2008	-1726	W 5
07-31	+2017	-2490	W 5
08-07	+1818	-1747	NW 7
08-14	+348	-25	W 5
08-21	-654	+824	SE 5
08-28	-1198	+816	E 4
09-04	-1110	-60	- 0
09-11	+1213	-2234	WSW 2
09-18	+1914	-2629	W 10
09-25	-10	+361	S 5
10-02	+919	-1777	NW 11
10-09	-166	+276	NE 8
10-16	+856	-1444	N 2
10-24	+362	-812	N 5
10-30	+148	+272	N 5
11-06	+1042	-1095	SW 1
11-13	+1051	-1164	SW 7
11-20	+273	+291	N 7
11-27	+220	-128	S 2
12-04	+552	-832	S 4
12-11	+1181	-1543	SW 5
12-18	+1298	+731	NW 4
12-27	+2223	-3143	WNW 5
1975-01-08	+1244	-1163	W 5
01-08	+1322	-1585	NW 5
01-15	+1272	-1545	W 5
01-22	+2055	-216	WSW 9
01-30	+826	+462	ESE 9
02-05	+2287	-2596	W 5
02-12	(Ice)	(Ice)	SW 2
02-19	+1644	-1866	W 9
02-26	+1419	-1463	W 8
03-05	-36	+265	- 0

Date	Transport, m^3/s Above main pycnocline	Below main pycnocline	Wind at 10 m above sea level, m/s
1975-03-12	-40	+1158	NE 4
03-20	+77	-18	N 4
03-26	-619	+596	E 1
04-02	+1780	-2005	W 7
04-09	-185	+290	
	Σ = +31560	Σ = -29007	
	Mv = +595	Mv = -547	

6. SUMMARY AND CONCLUSIONS

6.1 Summary of the Results

A numerical model has been developed to predict the effect of a planned nuclear power plant on the circulation of Bråviken estuary. Thermal waste in the form of heated water is to be discharged from the plant. The heated water is a source of buoyancy which can change the natural circulation. The numerical model uses the basic laws of hydrodynamics to predict the estuarine flow. The model prediction of the natural flow is used as a basis against which results from different heated water predictions are compared. Field work specifically designed to establish the validity of the prediction of that natural state was not included in this study. Field data was taken in another study in order to ascertain natural conditions near the intake-outlet. That project was intended to provide information for a nearfield hydraulic model. However, a few of the measurements from that study have been used to make a preliminary comparison with model results. To the extent that comparisons can be made, the numerical model represents the essential features of the known estuarine flow in Bråviken. Future field work may indicate areas of improvement in the model.

The natural conditions modelled represent two states of thermal stratification: summer with a strong vertical temperature gradient and winter with essentially no vertical temperature variation. These two states are established by imposing typical conditions on the net surface heat flux.

For each of these seasons, two different intake configurations have been considered: a surface intake, as is planned, and a bottom intake. In all cases the outlet is located at the surface and on the oceanic side of the intake. Several typical wind conditions have been considered: no wind, a steady wind of 5 m/s and a 12 m/s, time dependent wind which gradually builds from the west, shifts to the east and then dies. A series of experiments, under the winter conditions and with varying amounts of runoff, has also been conducted.

In the summer, a thermocline is developed due to an excess of incoming solar radiation. The surface temperature reached is about 19.6°C while the bottom temperature in the inner basin is about 10.1°C. Table I contains the mean values of salinity and temperature inside the sill as well as the net transport into Bråviken at the sill. The percent change from the "natural state" is given in parentheses. The average-temperature change is greatest, +28.6 %, with unfavorable wind conditions and a surface intake. However, with a bottom intake the average temperature change is less than 3 %. The surface intake receives water at about 20°C and the outlet returns it at about 30°C. This large increase in temperature causes a decrease in the basic estuarine circulation approaching 30 %. In contrast, the bottom intake receives water at about 5°C and the outlet releases it at the surface at about 15°C which is below the ambient temperature. The estuarine circulation is slightly increased (1 - 2 %).

In the winter there is little natural temperature stratification. Salinity stratification is maintained, as in the summer, by subsurface Baltic water flowing in under the more brackish water leaving at the surface. The runoff largely determines the salt stratification. Table II shows the winter values of mean temperature and salinity and net transport into Bråviken. The salinity change for a surface intake is on the order of 5 %. This is a salinity change of about 0.3 o/oo. For the time dependent wind it may be twice as much. The average temperature of the inner basin can change by almost +50 % with a variable wind and a surface intake. This is due to recirculation when the wind transports heated water from the outlet to the intake. The estuarine circulation can be reduced to almost nothing (-93.2 %). With the bottom intake, the situation is somewhat better but the estuarine circulation can still be decreased to one half of its natural state. Temperature increases are still quite significant at about 30 %. The salinity change is reduced to one half of that for the surface intake.

The winter conditions have been used for a series of runoff experiments with and without a surface intake. In this series, losses to the atmosphere were not considered so that the effect of increased runoff alone could be studied. Table III summarizes the results. Salinity decreases as runoff increases. The effect is about the same with or without the intake. The difference between the natural and surface intake salinity is from 6 % to 8 % for all runoff values. The change is less than 0.5 ppm. It should be noted, however, that this change is not small when the range of salinity, 5 - 7 ppm for the lowest runoff, is considered. The change in mean salinity is almost 25 % of the range of salinity. However, as the runoff is increased the range increases until it is about 1 - 7 ppm. A change in mean value of 0.3 ppm means a change of only 5 % of the natural range. The difference in the mean temperature with and without the intake ranges from +71.8 % with the lowest runoff to +4.4 % with the highest runoff. The decrease in the estuarine circulation ranges from -72.0 % at low runoff to -15.3 % at high runoff. The highest value of runoff comes from data taken during the last 40 years and is equal to the circulation through the cooling system of the proposed reactor.

6.2 Conclusions

With the construction of a bottom intake located at a depth of about 40 meters, there will be little noticeable effect on the circulation, temperature or salinity fields in Bråviken during the summer. In the summer the vertical heat stratification and the natural estuarine circulation make it possible to inject heated cooling water into the environment with little effect because the heated water discharged at the surface is below the ambient temperature.

However, in the winter the bottom intake offers only a partial improvement over a surface intake. During the winter the heated water would cause considerable disruption of the natural circulation, temperature and salinity of Bråviken. The bottom intake could cause changes of as much as 50 % in the natural state. The surface intake would cause changes of almost twice as much. The heated water causes sizable horizontal density gradients which are sufficient to counteract the weak natural flow.

The winter situation is improved if the runoff is large compared to the cooling water circulation. However, the reverse is true for the planned Tunaberg plant. The runoff can be as low as 25 m^3/s while the plant discharge is about 300 m^3/s. Time dependent wind experiments suggest that the average winter temperature and circulation are strongly affected for several weeks after a storm of a few days duration. The effect of a series of such storms would not only provide considerable environmental stress but would also tend to accumulate the effects if they occured within several weeks of each other, causing disruption of the natural conditions beyond those previously indicated.

As a recipient of heated cooling water from a large thermal power plant, Tunaberg does not seem to be a favorable site. The plant's location on the deep channel into Bråviken makes disturbance of the natural estuarine flow in Bråviken very likely.

Further studies with an integration of field experiments and model studies would be advisable to more critically determine the suitability of this site. The model has been further developed to include vertical mixing which is a function of the flow and density stratification.

Field measurements should be carried out together with numerical experiments using the more realistic form of vertical mixing.

Table 6.1. Summer conditions, runoff = 50 m^3/s

Case	Salinity o/oo (% Δ)	Temperature °C (% Δ)	Transport in m^3/s (% Δ)
No intake, τ=0	6.58 (0.0)	13.53 (0.0)	569. (0.0)
Surface intake, τ=0	6.50 (-1.2)	15.14 (+11.9)	428. (-28.3)
Bottom intake, τ=0	6.60 (+ .3)	13.78 (+1.8)	571. (+ .4)
Surface intake, τ(t)	6.47 (-1.8)	17.40 (+28.6)	439. (-22.8)
Bottom intake, τ(t)	6.61 (+ .5)	13.92 (+2.9)	583. (+2.5)

Table 6.2. Winter conditions, runoff = 50 m^3/s

Case	Salinity o/oo (% Δ)	Temperature °C (% Δ)	Transport in m /s (% Δ)
No intake, τ=0	6.46 (0)	4.61 (0)	279. (0)
Surface intake, τ=0	6.20 (-4.0)	6.04 (31.0)	19. (-93.2)
Bottom intake, τ=0	6.29 (-2.6)	5.56 (20.6)	140. (-49.8)
Surface intake, τ(t)	6.12 (-5.3)	6.78 (47.1)	75. (-73.1)
Bottom intake, τ(t)	6.26 (-3.1)	6.06 (31.5)	197. (-29.4)

Table 6.3. Runoff series, winter

	Salinity			Temperature			Transport		
Runoff	No intake	Surface intake	(% Δ)	No intake	Surface intake	(% Δ)	No intake	Surface intake	(% Δ)
50	6.46	6.08	(-5.9)	4.61	7.92	(+71.8)	279.	78.	(-72.0)
100	6.16	5.73	(-7.0)	4.95	6.81	(37.6)	416.	202.	(-51.4)
150	5.91	5.44	(-8.0)	4.28	5.55	(29.7)	470.	316.	(-32.8)
200	5.71	5.28	(-7.5)	4.08	4.72	(15.7)	521.	402.	(-22.8)
250	5.54	5.18	(-6.5)	3.96	4.27	(7.8)	559.	464.	(-17.0)
300	5.39	5.03	(-6.7)	3.86	4.02	(4.4)	588.	498.	(-15.3)

REFERENCES

Arakawa, A. (1966): Computational design for long-term numerical integration of the equations of fluid motion: I. Two-dimensional incompressible flow, J. of Comp. Physics, Vol. 1, No. 1, pp. 392-405

Ehlin et. al. (1974): Kylvatteneffekter på miljön. Vattenfalls miljövårdsstiftelse, Statens Naturvårdsverk, Publikationer 1974:25

Fisher, G. (1965): A survey of finite-difference approximations to the primitive equations, Mon. Weather Rev., Vol. 93, No. 1, pp. 1-10

Fredrich, H., Levitus, S. (1972): An approximation to the equation of state for sea water, suitable for numerical ocean models, J. of Ph. Oceanography, Vol. 2, No. 4

Grammeltvedt, A. (1969). A survey of finite-difference schemes for the primitive equations for a barotropic fluid, Mon. Weather Rev., Vol. 97, No. 5, pp. 384-404

Kurihara, Y. (1965): On the use of implicit and iterative methods for the time integration of the wave equation, Mon. Weather Rev., Vol. 93, No. 1, pp. 33-46

Lilly, D. K. (1965): On the computational stability of numerical solutions of time-dependent non-linear geophysical fluid dynamics problems, Mon. Weather Rev., Vol. 93, No. 1, pp. 11-26

Milanov, T (1969): Avkylningsproblem i recipienter vid utsläpp av kylvatten. Notiser och preliminära rapporter, Serie Hydrologi, No. 6

Ogura, Y., Yagihashi, A. (1969): A numerical study of convection rolls in a flow between horizontal parallel plates, J. of the Met. Soc. of Japan, Vol. 47, No. 3, pp. 205-217

Piacsek, S.A., Williams, G. P. (1970): Conservation properties of convection difference schemes, J. of Comp. Phys., Vol. 6, pp. 392-405

Pritchard, D. W. (1956): The dynamic structure of a coastal plain estuary, J. Marine Res., Vol. 15, pp. 33-42

---- (1958): The equations of mass continuity and salt continuity in estuaries, J. Marine Res., Vol. 17, pp. 412-423

Shuman, F. G. (1962): Numerical experiments with the primitive equations, Proceedings of the International Symposium on Numerical Weather Prediction in Tokyo, November 1960, Meteorological Society of Japan, Tokyo, Mar. 1962, pp. 85-107

Stewart, R. W. (1957): A note on the dynamic balance for estuarine circulation, J. Marine Res., Vol. 16, pp. 34-39

Young, J. A. (1968): Comparative properties of some time differencing schemes for linear and nonlinear oscillations, Mon. Weather Rev., Vol. 96, No. 6, pp. 357-364

Notiser och preliminära rapporter

Serie HYDROLOGI

Nr 1 Sundberg-Falkenmark, M
Om isbärighet. Stockholm 1963

Nr 2 Forsman, A
Snösmältning och avrinning. Stockholm 1963

Nr 3 Karström, U
Infrarödteknik i hydrologisk tillämpning: Värmebilder som hjälpmedel i recipientundersökningar. Stockholm 1966

Nr 4 Moberg, A
Svenska sjöars isläggnings- och islossningstidpunkter 1911/12-1960/61. Del 1. Redovisning av observationsmaterial. Stockholm 1967

Nr 5 Ehlin, U & Nyberg, L
Hydrografiska undersökningar i Nordmalingsfjärden. Stockholm 1968

Nr 6 Milanov, T
Avkylningsproblem i recipienter vid utsläpp av kylvatten Stockholm 1969

Nr 7 Ehlin, U & Zachrisson, G
Spridningen i Vänerns nordvästra del av suspenderat materiel från skredet i Norsälven i april 1969. Stockholm 1969

Nr 8 Ehlert, K
Mälarens hydrologi och inverkan på denna av alternativa vattenavledningar från Mälaren. Stockholm 1970

Nr 9 Ehlin, U & Carlsson, B
Hydrologiska observationer i Vänern 1959-1968 jämte sammanfattande synpunkter. Stockholm 1970

Nr 10 Ehlin, U & Carlsson, B
Hydrologiska observationer i Vänern 17-21 mars 1969. Stockholm 1970

Nr 11 Milanov, T
Termisk spridning av kylvattenutsläpp från Karlshamnsverket. Stockholm 1971

Nr 12 Persson, M
Hydrologiska undersökningar i Lappträskets representativa område. Rapport I. Stockholm 1971

Nr 13 Persson, M
Hydrologiska undersökningar i Lappträskets representativa område. Rapport II: Snömätningar med snörör och snökuddar Stockholm 1971

Nr 14 Hedin, L
Hydrologiska undersökningar i Velens representativa område. Beskrivning av området, utförda mätningar samt preliminära resultat. Rapport I. Stockholm 1971

Nr 15 Forsman, A & Milanov, T
Hydrologiska undersökningar i Velens representativa område. Markvattenstudier i Velenområdet. Rapport II. Stockholm 1971

Nr 16 Hedin, L
Hydrologiska undersökningar i Kassjöåns representativa område. Nederbördens höjdberoende samt kortfattad beskrivning av området. Rapport I. Stockholm 1971

Nr 17 Bergström, S & Ehlert, K
Stochastic Streamflow Syntheses at the Velen representative Basin. Stockholm 1971

Nr 18 Bergström, S
Snösmältningen i Lappträskets representativa område som funktion av lufttemperaturen. Stockholm 1972

Nr 19 Holmström H
Test of two automatic water quality monitors under field conditions. Stockholm 1972

Nr 20 Wennerberg, G
Yttemperaturkartering med strålningstermometer från flygplan över Vänern under 1971. Stockholm 1972

Nr 21 Prych, A
A warm water effluent analyzed as a buoyant surface jet. Stockholm 1972

Nr 22 Bergström, S
Utveckling och tillämpning av en digital avrinningsmodell. Stockholm 1972

Nr 23 Melander, O
Beskrivning till jordartskarta över Lappträskets representativa område. Stockholm 1972

Nr 24 Persson, M
Hydrologiska undersökningar i Lappträskets representativa område. Rapport III: Avdunstning och vattenomsättning. Stockholm 1972

Nr 25 Häggström, M
Hydrologiska undersökningar i Velens representativa område. Rapport III: Undersökning av torrperioderna under IHD-åren fram t o m 1971. Stockholm 1972

Nr 26 Bergström, S
The application of a simple rainfall-runoff model to a catchment with incomplete data coverage. Stockholm 1972

Nr 27 Wändahl, T & Bergstrand, E
Oceanografiska förhållanden i svenska kustvatten. Stockholm 1973

Nr 28 Ehlin, U
Kylvattenutsläpp i sjöar och hav. Stockholm 1973

Nr 29 Andersson, U-M & Waldenström, A
Mark- och grundvattenstudier i Kassjöåns representativa område. Stockholm 1973

Nr 30 Milanov, T
Hydrologiska undersökningar i Kassjöåns representativa område. Markvattenstudier i Kassjöåns område. Rapport II. Stockholm 1973

SMHI Rapporter

HYDROLOGI OCH OCEANOGRAFI

Nr RHO 1. Weil, J G
Verification of heated water jet numerical model
Stockholm 1974

Nr RHO 2 Svensson, J
Calculation of poison concentrations from a hypothetical accident off the Swedish coast
Stockholm 1974

Nr RHO 3 Vasseur, B
Temperaturförhållanden i svenska kustvatten
Stockholm 1975

Nr RHO 4 Svensson, J
Beräkning av effektiv vattentransport genom Sunninge sund till Byfjorden
Stockholm 1975

Nr RHO 5 Bergström S & Jönsson, S
The application of the HBV runoff model to the Filefjell research basin
Norrköping 1976

Nr RHO 6 Wilmot, W
A numerical model of the effects of reactor cooling water on fjord circulation
Norrköping 1976